Sains Malaysiana 46(11)(2017): 2101-2108
http://dx.doi.org/10.17576/jsm-2017-4611-10

Shear Strength of Cemented Sand Gravel and Rock Materials
(Kekuatan Ricih Pasir Kerikil Bersimen dan Bahan Batu)

ZHONGWEI LIU*, JINSHENG JIA, WEI FENG, FENGLING MA & CUIYING ZHENG

ABSTRACT

Shear strength is currently a significant parameter in the design of cemented sand gravel and rock (CSGR) dams. Shear strength tests were carried out to compare material without layers noumenon and layer condition. The experimental results showed good linearity in the curves of shear strength and pure grinding tests with correlation coefficients of nearly 97%. The friction coefficient was similar to that of C10 roller-compacted concrete (RCC), but the cohesion value was weaker than that of RCC. The shear strength of the CSGR layers decreased by 40% when retarding mixtures were not added and the layer was paved immediately after 4 h of waiting interval.

Keywords: Cohesion; CSGR; friction; layer; shear strength

ABSTRAK

Kekuatan ricih merupakan parameter penting dalam reka bentuk pasir kerikil bersimen dan batu empangan (CSGR). Ujian kekuatan ricih dilakukan untuk membandingkan bahan tanpa lapisan noumenon dan keadaan berlapis. Keputusan eksperimen menunjukkan garis lurus yang baik dalam lengkungan kekuatan ricih dan ujian pengisaran tulen dengan pekali korelasi menghampiri 97%. Pekali geseran adalah sama dengan penggelek konkrit yang dipadatkan C10 (RCC), tetapi nilai kejeleketan lebih rendah berbanding RCC. Kekuatan ricih lapisan CSGR menurun sebanyak 40% apabila campuran perencat tidak ditambah dan lapisan itu diturap dengan serta-merta selepas selang masa 4 jam.

Kata kunci: CSGR; geseran; kejeleketan; kekuatan ricih; lapisan

INTRODUCTION

Cemented sand gravel and rock (CSGR) dams are a new type of dams that combine the advantages of roller-compacted concrete (RCC) dams and concrete-face rock-fill dams (CFRD) (Jia et al. 2016). The key factor in CSGR dam design is anti-slide stability (China Standard SL678 2014). Specifically, shear strength parameters like the friction coefficient and the cohesive force are directly related to the optimization of section configuration (Farinha et al. 2015). The shear strength parameters of CSGR dams may refer to: A roller compacted dam (RCD) (Park et al. 2007) go; A lean RCC dam (Gouvas & Orfanos 2014); A grout-enriched vibratable RCC dam (GEVR); and a medium mortar RCC dam (Asmida et al. 2017; Shi & Fang 2006). The RCD method was developed in Japan (Schrader 1977) and mainly follows the column method of a conventionally vibrated concrete (CVC) dam, including construction joint curing, surface roughening, cleaning and paving mortar. The amount of cement is about 120 kg/m^3 for 1 m^3 with inter-laminar shear cohesive forces of 2.5-3.0 MPa. Both Shimajigawa and Okawa Dams are typical examples (Nagataki et al. 2008). Lean RCC dams are derived from the concept of earth-rock dam construction (Gouvas & Orfanos 2014). Without layer treatment, the amount of cement is 60-120 kg/m^3 and the inter-laminar shear cohesive force is 2.5-3.0 MPa. Examples include the Willow Creek Dam and the Monkesville Dam in USA. GEVR dams like the Upper Stillwater Dam have cement amounts above 250 kg/m^3 with fly ash additive of 70%. The design principle is to preserve the high density of the concrete and maintain layer cohesion above 2.2 MPa while avoiding layer treatment (Huan et al. 2005). For a medium mortar RCC dam, the amount of cementitious materials is 140-160 kg/m^3 and the cohesive force of the interlayer drops to 0.8-1.4 MPa (Cervera et al. 2000). Compared to a CVC dam, the construction characteristics of a CSGR dam include continuous pouring and the absence of a longitudinal joint. The amount of horizontal bedding is more than that in normal concrete, while the slice thickness is larger compared to that of RCC dams (China Standard SL678 2014). At the same time, the properties of CSGR dams are similar to those lean RCC dams, but the construction method resembles that of regular RCC. Also, it needs to be treated if the layer does not meet requirements. Generally, the cushion material for RCC dam surfaces uses mortar, cement paste, or first grade RCC. In China and abroad, there have been few studies regarding the appropriate time interval for CSGR dam layers. Based on the successful results of anti-shear parameters and layer mixtures on RCC dams, studies regarding anti-shear parameters and evaluations of CSGR dams would be valuable. The shear strength test method for RCC could be applied to CSGR measurements. Many test methods already exist for RCC and CVC materials. The most common method is the direct shear test (Carvajal et al. 2009; Oyanguren et al. 2008; Wang et al. 2016, 2013) which can be divided into the horizontally pushing method, the oblique pushing method and the wedge method. The two pushing-based shear test methods are the most commonly used cemented interfaces between concrete and bedrock, soft intercalated layers in rock mass, concrete layers and concrete without layers.

Two types of problems related to shear strength testing instruments exist. The first is the change in constant vertical stress caused by dilatation of the concrete specimen under shear load. The second is the inaccuracy of the friction coefficient correction on shear apparatus rollers. All of these can lead to inaccuracies in experimental measurements. This work utilizes a newly developed shear test apparatus that can maximize the testing accuracy while mitigating the previously described problems.

Materials and Methods

DESIGN METHODS OF CSGR MIX RATIO

In principle, the sandy gravel and rocks does not need classification, but screening tests are first done to natural materials in the mix ratio design and the coarsest gradation, the finest gradation and average gradation of aggregate are distinguished (Feng et al. 2013; John et al. 2017). The sand rate range should be controlled at 25%-30%. Sand gravel was a kind of natural mixture material whose diameter was under 2 cm. Rocks' diameter shown in this paper was between 2 and 15 cm. The granulometric of sand gravel and rock was shown in Table 1. Meanwhile, natural sandy gravels are distributed in the particle size range of the most coarse and finest. The sand gravel in above gradation is chosen in the experiments. CSGR strength test are conducted with different water consumption shown in Figure 1. According to the relationship of water consumption and strength, appropriate water consumption range and responding strength range are confirmed, that means water consumption and strength vary with aggregate gradation. If there is no obvious difference in aggregate gradation, average gradation is chosen as the experiment object. That is similar to 'point' control mode of concrete strength fixed by aggregate gradation and water consumption, but the gradation was still not fixed and its deviation was higher than concrete strength, so the mix ratio should obey the 'line' control mode shown in Figure 2. Also, it needs to guarantee minimum value of average gradation sandy gravels strength meet configuration strength, namely 'single with single strength provisions of principle'. If gradation has a great change, in order to ensure a representative sandy gravel of CSGR strength meet the design requirements and higher reliability, the minimum value of average gradation strength reflected the condition of overall gradation is suitable to configuration strength responding to the most water amount, located in the appropriate range. Meanwhile, the minimum value of finest gradation strength should not be less than the design strength, that is 'double-graded stipulate the principle of double strength'. The design compressive strength of CSGR refers to the standard value with reliability at 80%, which is measured by the standard test method with cube in length of 150 mm, curing 180 days. The CSGR configuration strength is calculated as formula:

$$f_{cu,\sigma} = f_{cu,k} + t\sigma \quad , \tag{1}$$

where $f_{cu,o}$ is the CSGR configuration strength, *MPa*; $f_{cu,k}$ is the standard value of design strength of CSGR for curing 180d, MPa; t is the probability coefficient, chosen by reliability P. According to hydraulic concrete, P is 80% generally and the corresponding t is 0.842; and σ is the standard deviation of CSGR compressive strength, *MPa*.

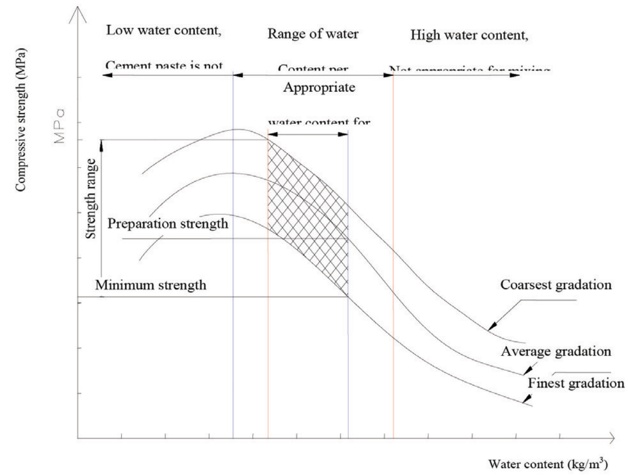

FIGURE 1. Relationship between CASR compressive strength and water consumption under different gradation

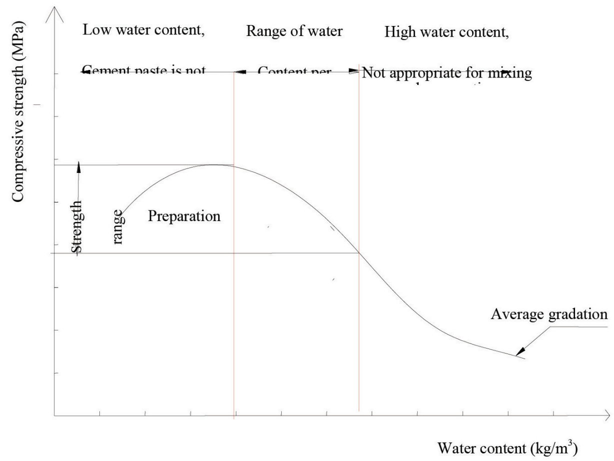

FIGURE 2. Relationship between CASR compressive strength and water consumption under average gradation

TABLE 1. Granulometric of sand gravel and rock

	Rock				Sand gravel					
Diameter (mm) No.	150 ~ 80	80 ~ 40	40 ~ 20	20 ~ 5	5 ~ 2.5	2.5 ~ 1.25	1.25 ~ 0.63	0.63 ~ 0.315	0.315 ~ 0.158	<0.158
1#	24.4	21.0	16.5	17.0	1.5	1.3	1.1	6.4	3.6	7.2
2#	31.1	22.2	24.0	10.0	1.6	1.0	0.7	3.6	1.8	4.1
3#	20.0	20.2	18.1	17.0	2.5	2.3	1.7	5.2	3.4	9.6
4#	20.0	26.6	17.2	15.1	1.5	1.2	1.0	3.6	4.1	9.7
5#	25.5	23.5	22.5	7.4	1.1	1.1	0.9	6.1	3.2	8.9
6#	22.8	25.0	17.6	11.7	1.2	1.1	1.3	6.9	3.5	8.9
7#	22.2	30.9	14.6	8.9	0.6	0.6	0.6	4.1	5.7	12.0
8#	21.7	29.0	20.1	6.7	0.1	0.3	0.1	3.7	4.9	13.3
9#	23.8	40.1	13.1	3.2	0.3	0.6	0.7	4.4	4.4	9.4
Average percentage (%)	23.5	26.5	18.2	10.8	1.1	1.0	0.9	4.9	3.8	9.2
The coarse gradation envelope (%)	31.1	32.8	13.4	10.0	1.6	1.0	0.7	3.6	1.8	4.1
The finest gradation envelope (%)	20.0	20.3	18.1	17.0	1.8	0.6	0.3	3.7	4.9	13.3

TABLE 2. Mix ratio parameters of CSGR

No.	Water binder ratio	Water cement ratio	Water consumption (kg/m^3)	Cementitious materials (kg/m^3)	Sand gravel (kg/m^3)	Rock (kg/m^3)	VC (s)	Density of full grade specimen (kg/m^3)	Density of wet sieve specimen (kg/m^3)	Relative density (%)
A1	0.9	1.8	72	80	584	1816	7	2543	2479	99.6
A2	1.68	3.35	134	80	934	1292	-	2441	-	-

TABLE 3. The test results of CSGR compressive strength

No.	Compressive strength of cubic specimens (MPa)								
	150 mm			300 mm			450 mm		
	28 d	90 d	180 d	28 d	90 d	180 d	28 d	90 d	180 d
A1	6.7	10.2	14.1	6.2	9.8	11.9	6.0	9.2	11.1
A2	3.6	5.2	7.1	3.2	4.6	5.8	2.7	4.1	5.3

Experimental details

Materials

Sand gravel was a kind of natural mixture material digged from the river bed whose diameter was under 2 cm. Rocks diameter shown in this paper was between 2 and 15 cm. The mixed proportions of the two materials used in the shear tests of CSGR without layers are listed in Table 2. The results of compressive strength tests are shown in Table 3. The first group was named A1 with 40 kg/m^3 each of cement and fly ash, respectively. Ordinary Portland cement of 42.5 was obtained from Taihang Qianjing Co., Ltd in Beijing. Grade II fly ash was selected from Xuanwei. Sand gravel and rocks were derived from gravel and pebbles around the Yongding River in Beijing. The second test group was named A2 and used 50 and 30 kg/m^3 of cement and fly ash, respectively. Ordinary Portland cement of 42.5 was obtained from Jidong Co., Ltd in Hebei. Grade II fly ash was selected from the Datong thermal power plant. Sand gravel and rocks were taken from Shoukoubu CSGR dam in Shanxi. Properties of the fly ash were tested and shown in the Table 4 (Das & Yudhbir 2005; DL/T 5055 2007).

TABLE 4. Properties of the fly ash

Item	Fineness degree (45μm sieve residue)	Ratio of water demand (%)	Loss on ignition (%)	Water content (%)	SO_3 (%)	f-CaO (%)	Stability
Test values	22.1	98	7.6	0.8	2.3	0.8	Qualified

The initial setting times of the two ratios of CSGR were 7 h each and the penetration resistances were about 14 MPa. When the penetration resistance was reduced to 6 MPa, the corresponding time was decreased to 5 h. From the RCC construction experience, the initial setting was not long enough for continual placing. Accordingly, the value should be 4 h, which was corresponding to time that the penetration resistance was down to 5-6 MPa. Shear strength tests on CSGR layers were conducted based on the shear tests of group A2. The interval time was 4 h.

DESIGN

Cubes with dimensions of 150 mm^3 were molded in one step and used for CSGR shear strength tests.

The shear specimen for interlayer bonding required two molding steps, but employed the same specimen size. Mixtures for CSGR were formulated according to the A2 ratio in Table 2. Half of the specimen height was set into the mold, which resulted in a CSGR with a height of 75 mm. The specimen was half of the mold height after compacting and was then kept in the curing room for 4 h. The same procedures were followed for the other half of the specimen. The mold was removed for layer surface treatments, which included removing the scum with an air gun and roughening to expose aggregates. Then, the top half was molded and cured for 170 days. Finally, 15 specimens were taken in one group for tests. A concrete shear tester designed by the China Institute of Water Resources and Hydropower Research (WHY-500/1000) was used for testing as in Figure 3. Calculations and analysis of the horizontal and vertical load distributions while cutting and rubbing indicate that the loading from two directions were located on one section. This result could effectively eliminate the destructive effect of compression-shear damage between shear processes while assuring the reliability of these results.

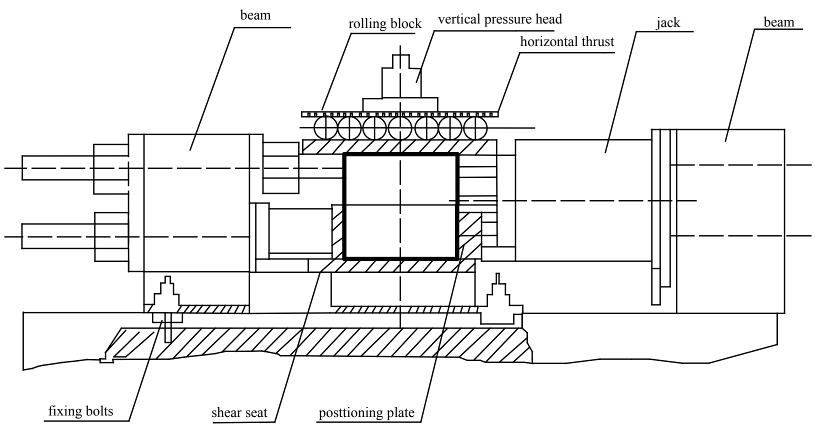

FIGURE 3. The structure chart of horizontal load device in shear test

The shear tests of CSGR without layers and the layer shear tests of A2 were conducted with two mix proportions. Both determined the maximum normal stress to be 2.0 MPa, which was imposed by 4 grades, with 3 samples in each grade. The shear strength is commonly defined by the Mohr-Coulomb failure equation (China Standard SL352 2006).

$$\tau = \sigma f' + c' \,, \tag{2}$$

where τ is the shear strength, Mpa; σ is the normal stress, Mpa; f′ is the friction coefficient; c′ is the cohesion, Mpa; f′ and c′ were obtained by shear strength test with f′ is the tgα (slope of a straight line); and c′ is the intercept.

Results and Discussion

SHEAR STRENGTH TESTS OF CSGR

The shear test results indicated that the normal and shear stress were in the same section, which can help eliminate shear-compression failure while improving test precision. During the shear process, the normal stress was constant and the normal and shear forces crossed the shear plane center. Figure 4 shows the shearing position of specimens. Specimens were all split by half along the long axis with little coarse aggregate splitting, while the section was 10-20 mm ups and downs. The shear failure stress increased with the increase of normal stress. The shear strength

(a) The shear strength tests of CSGR

(b) Fluctuation measurements of shearing section of CSGR noumenon

FIGURE 4. The shear strength tests of CSGR

TABLE 5. Shear strength parameters comparison of CSGR and concrete (Zhou & Dang 2011)

Category name	Features	Mean value M_f`	Variation coefficient Δ_f`	Standard values f `	Mean value $\mu_{c`}$ (MPa)	Variation coefficient $\Delta_{c`}$	Standard values (MPa) c`	Notes
Roller compacted concrete (RCC)	Ratio of cementitious materials at 180 d age	1.1-1.3	0.21	0.91-1.07	1.73-1.96	0.36	1.21-1.37	
Conventionally vibrated concrete (layer adhesion)	90 d C10-C20	1.3-1.5	0.20	1.08-1.25	1.60-2.00	0.33	1.16-1.45	
A1	120d, Shear strength tests			1.45			1.44	Initial setting time 7(h)
	120d, Pure grinding tests			1.16			0.64	
A2	90 d, Shear strength tests			0.89			0.82	Initial setting time 7(h)
	90 d, Pure grinding tests			0.62			0.64	
A2-4	170d, Shear strength tests			1.08			0.44	Initial setting time 4(h)
	170 d, Pure grinding tests			0.68			0.19	

The proportion of cementitious materials was above 150 kg/m^3

parameters comparison of CSGR and concrete were shown in Table 5. Table 3 indicates that the compressive and splitting tensile strengths of A1 after 90 d were 10.2 and 0.8 MPa, respectively. The correlations between the shear stress curves in Figure 5(a) correspond to different normal stresses and were in good agreement. The correlation coefficients exceeded 97%. The shear strength test yielded a friction coefficient of 1.45 and a cohesion of 1.44 MPa. This value was 13% of the compressive strength and 1.8 times the splitting tensile strength. When the friction coefficient dropped by 20% to 1.16, the cohesion also decreased by 55% to 0.64 MPa. This corresponds to 5.7% of the compressive strength and 0.8 times the splitting tensile strength.

Table 3 indicates that the compressive and splitting tensile strengths of A2 after 90 days were 4.9 and 0.4 MPa, respectively. The shear stress curves in Figure 5(b) corresponding to different normal stresses also had strong correlation. Correlation coefficients were in excess of 99.8%. The shear strength test yielded a friction coefficient of 0.89 and a cohesion of 0.82 MPa. This value was 17% of the compressive strength and twice the splitting tensile strength. For pure grinding tests, the friction coefficient dropped 30% to 0.62 and the cohesion also decreased by 22% to 0.64 MPa. This corresponds to 13% of the compressive strength and 1.6 times the splitting tensile strength.

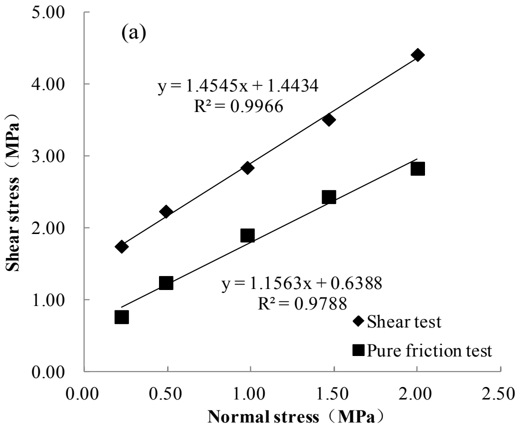

(a) Test group A1

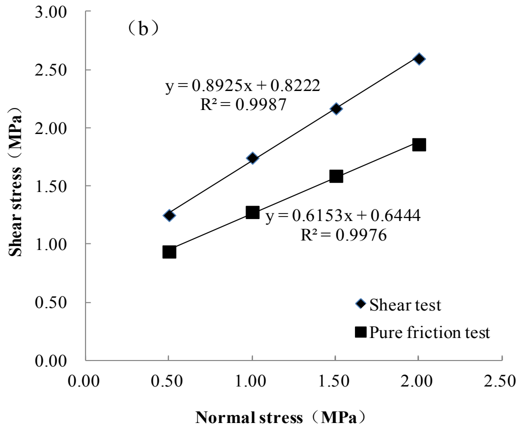

(b) Test group A2

FIGURE 5. The correlation curves of σ-τ under normal stress

THE SHEAR STRENGTH OF CSGR LAYER

During the placing and spreading processes of construction, layers will inevitably exist with different working conditions due to intermittent work or downtimes. For this reason, studies regarding layer shear strength, rational control over time intervals of construction, surface treatment and other measures, are very important. The shear strength and pure grinding tests curves are shown in Figure 6. Retarding water-reducer admixtures were often used in RCC dam construction to extend layer time intervals, increase binding force and other factors. However, no additives were used in the CSGR in this work, which resulted in short initial setting times. Even if the interval time was only 4 h, the combination of upper and lower layers was still weak. When the interval time of CSGR was 4 h, the compressive and splitting tensile strengths of group A2-4 were 6.5 and 0.4 MPa, respectively. There was a strong linear correlation for the anti-shear and pure grinding tests. Results of shear strength tests in Figure 6 show a friction coefficient of 1.08 and a cohesion of 0.44 MPa. This value was 7% of the compressive strength and 1.1 times the splitting tensile strength. For the pure grinding tests, the friction coefficient decreased by 37% to 0.68, the cohesion also decreased by 57% to 0.19 MPa. This corresponds to only 3% of the compressive strength and 0.5 times the splitting tensile strength. The compressive strength and friction coefficients of CSGR with interval times of 4 h increased by 25% and 21%, respectively. Separately, the cohesion decreased by 46%.

The tensile and shear strengths of RCC were lower, owing to the weak plane of the RCC material. The shear strength parameter was significantly influenced by the amount of cementitious materials, the layer interval time, layer treatment and age. These conclusions were determined through statistical analyses of the test methods. The experimental shearing data for RCC dams were compared and analyzed in combination with the statistical data of shear parameters in the joint surface of CVC. As shown in Table 5, the concrete shear strength parameters were given in ‘DL 5108-1999 design specification for concrete gravity dams’. The CSGR friction coefficient was close to RCC C10 and CVC, but the cohesion value was weaker than RCC (Khan et al. 2017; Zhou & Dang 2011). Some studies have shown that the RCC properties with layers were lower than the noumenon value. Also, longer interval times resulted in decreased shear strength. CSGR materials observed the same trend (Song et al. 2012; Yuan et al. 2005). The fluctuation difference was obvious for the 4 h interval after observing the destruction conditions of CSGR. The results of layer shear tests showed the plasticity degree of the mortar was similar to the effect of embedding and cementation. Increasing the rolling times caused the mixtures to gradually liquefy, the grout of the cementitious materials floated and the plasticity layer was formed. If CSGR was paved before the pulp layer was formed, after rolling, the effects of cementation, embedding and meshing were more pronounced due to increased continuity between layers. That caused the submerge of CSGR aggregate via liquefaction. The aggregate could not sink into the grout under vertical vibration when being rolled, if the CSGR was paved on the grout after grout condensation. In fact, the continuity between layers was worse. As a result, the condensation state directly affects the performance of the cement layer. The shear performance tests indicate that the layer shear strength also fell by over 40% with a 4 h interval if no retarding admixtures were added. Based on these results, mixing CSGR with retarding admixtures may extend layer intermission time and guarantee layer dampening. Surface treatments such as spraying and roughening could be used to improve the binding properties before CSGR was placed and spread.

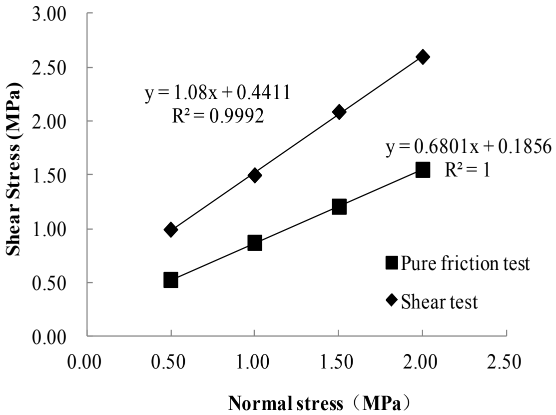

FIGURE 6.The shear strength and pure grinding tests curves of CSGR A2-4

Conclusion

The results of two types of shear strength experiments for CSGR indicate that the new device at the China Institute of Water Resources and Hydropower Research meets the test requirements. In shear strength tests, the friction coefficient of CSGR at the Shoukoubu dam in Shanxi province was 0.89 with a cohesion of 0.82 MPa. For the pure grinding test, the friction coefficient decreased 30% to 0.62 and cohesion decreased 22% to 0.64 MPa. The CSGR friction coefficient was similar to RCC, but the cohesion value was weaker. With a 4 h interval time, shear test results indicated the friction coefficient was 1.08 and the cohesive force was 0.44 MPa. However, for pure grinding tests, the friction coefficient was decreased by 37% to 0.68 and the cohesive force decreased by 57% to 0.19 MPa.

The cementing properties were directly influenced by the condensation conditions of the layer slurries. The results indicated that the layer shear strength also fell by over 40% with 4 h interval times when retarding admixture were absent. As such, retarding admixtures should be added to CSGR material. Additional surface treatment methods like spraying and roughening or others should be conducted prior to placing and spreading CSGR in order to enhance the layer bonding properties.

Acknowledgements

This work was supported by the National Basic Research Program (973 Program) of China (Grant No. 2013CB035903) and by the National Key Technology R&D Program (Grant No. 2013BAB06B02).

References

Asmida, I., Noor Akmal, A.B., Ahmad, I. & Sarah Diyana, M. 2017. Biodiversity of macroalgae in Blue Lagoon, the Straits of Malacca, Malaysia and some aspects of changes in species composition. *Sains Malaysiana* 46(1): 1-7.

Carvajal, C., Peyras, L., Bacconnet, C. & Becue, J. 2009. Probability modelling of shear strength parameters of RCC gravity dams for reliability analysis of structural safety. *European Journal of Environmental and Civil Engineering* 13(1): 91-119.

Cervera, M., Oliver, J. & Prato, T. 2000. Simulation of construction of RCC dams. II: Stress and damage. *Journal of Structural Engineering-asce* 126(9): 1062-1069.

Das, S.K. & Yudhbir. 2005. Geotechnical characterization of some indian fly ashes. *Journal of Materials in Civil Engineering* 17(5): 544-552.

DL/T 5055. 2007. *Technical Specification of Fly Ash for Use in Hydraulic Concrete.* Beijing: China Electric Power Press.

Farinha, M.L., Caldeira, L.M. & Neves, E.M. 2015. Limit state design approach for the safety evaluation of the foundations of concrete gravity dams. *Structure and Infrastructure Engineering* 11(10): 1306-1322.

Feng, W., Jia, J.S. & Ma, F.L. 2013. Study on design parameters of mix proportion forcemented sand and gravel (CSG). *Water Resources and Hydropower Engineering* 44(2): 55-58.

Gouvas, H. & Orfanos, C. 2014. Determination of factors affecting compressive strength of lean RCC mixtures: The experience of Filiatrinos Dam. *Geotechnical and Geological Engineering* 32(5): 1317-1327.

Jia, J., Liu, N., Zheng, C., Ma, F., Du, Z. & Wang, Y. 2016. Studies on cemented material dams and its application. *Journal of Hydraulic Engineering* 47(3): 315-323.

John, A., Hassan, B., Nur Hanisa, S., Kamaruzzaman, M. & Kadhar Sha, B.Y. 2017. Community structure and post-monsoonal distribution of icthyoplankton in Kuatan river, Malaysia. *Environment Ecosystem Science* 1(1): 01-03.

Khan, A., Rehman, R., Rashid, H. & Nasir, A. 2017. Exploration of environmental friendly adsorbents for treatment of azo dyes from textile wastewater and its dosage optimization. *Earth Science Pakistan* 1(1): 05-07.

Nagataki, S., Fujisawa, T. & Kawasaki, H. 2008. State of art of RCD Dams in Japan. Anais do 50° Congresso Brasileiro do Concreto CBC2008-RCC *Symposium Setmbro.* pp. 1-20.

Oyanguren, P.R., Nicieza, C.G., Fernandez, M.I. & Palacio, C.G. 2008. Stability analysis of Llerin Rockfill Dam: An *in situ* direct shear test. *Engineering Geology* 100(3): 120-130.

Park, C., Yoon, J., Kim, W. & Won, J. 2007. Mechanical and durability performance of roller-compacted concrete with fly ash for dam applications. *International Journal of Concrete Structures and Materials* 1(1): 57-61.

Schrader, E.K. 1977. Roller-compacted concrete. *Materials & Structures* 34(7): 413-417.

Shi, Y. & Fang, K.H. 2006. Strength of roller compacted concrete. *Key Engineering Materials* 302-303(6): 398-402.

Song, Y.P., Wen, W. & Wang, H.L. 2012. Analysis on compression-shear strength of roller compacted concrete. *Journal of Water Resources and Architectural Engineering* 6: 44-47.

SL352. 2006. *Test Code for Hydraulic Concrete.* Beijing: China Waterpower Press.

SL678. 2014. *Technical Guidelines for Cemented Material Dams.* Beijing: China Waterpower Press.

Wang, J., Yang, Y. & Chai, H. 2016. Strength of a roller compacted rockfill sandstone from *in-situ* direct shear test. *Soil Mechanics and Foundation Engineering* 53(1): 30-34.

Wang, W., Kou, S. & Xing, F. 2013. Deformation properties and direct shear of medium strength concrete prepared with 100% recycled coarse aggregates. *Construction and Building Materials* 48: 187-193.

Yuan, C.H., Zhou, J. & Min, H. 2005. An experiment study of shearing strensth of roller compacted concrete (RCC). *Soil Engineering and Foundation* 19(5): 68-71.

Huan, Z.Q., Song, Y.P. & Wu, Z.M. 2005. Numerical simulation of tensile failure at adjacent concrete layers in RCC dams. *Journal of Hydraulic Engineering* 6: 680-686, 693.

Zhou, J.P. & Dang, L.C. 2011. *Hydraulic Design Manual. 5th Volume of Concrete Dams*. Beijing: China Waterpower Press. p. 380.

Division of Materials
China Institute of Water Resources and Hydropower Research
Beijing 100038
China

*Corresponding author; email: lzw9958@163.com

Received: 8 January 2017
Accepted: 4 June 2017